C–S/C–Br metathesis enabled by an Au–Pd alloy nanoparticle catalyst

Takehiro Matsuyama,[1] Takafumi Yatabe,[1,2,*] and Kazuya Yamaguchi[1,3,*]

[1]Department of Applied Chemistry, School of Engineering, The University of Tokyo, 7-3-1 Hongo, Bunkyo-ku, Tokyo 113-8656, Japan.

[2]Precursory Research for Embryonic Science and Technology (PRESTO), Japan Science and Technology Agency (JST), 4-1-8 Honcho, Kawaguchi, Saitama 332-0012, Japan.

[3]Lead contact.

[*]e-mail: kyama@appchem.t.u-tokyo.ac.jp, yatabe@appchem.t.u-tokyo.ac.jp

GRAPHICAL ABSTRACT

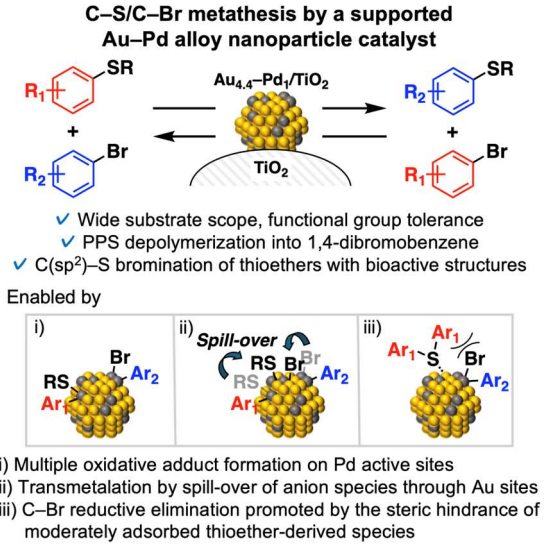

SUMMARY

Metathesis via C–S bond oxidative addition and reductive elimination has recently witnessed considerable development as a functionalization of ubiquitous sulfur-containing molecules with the molecular frameworks intact. Despite the synthetic utilities, C–S/C–Br metathesis has not been reported so far because of the difficulties in managing both reversible C–Br oxidative addition/reductive elimination and sterically sensitive transmetalation between the oxidative adducts. Herein, we report C–S/C–Br metathesis between thioethers and bromoarenes enabled by an Au–Pd alloy nanoparticle catalyst with a high Au/Pd ratio via utilization of unique multiple adsorption/active sites. This catalytic system was applicable to different thioethers and bromoarenes to afford both metathesis products in high yields, and late-stage bromination of C–S bonds in various thioethers possessing bioactive structures and depolymerization of polyphenylene sulfide to 1,4-dibromobenzene were also demonstrated.

INTRODUCTION

Metathesis, a reaction that involves the exchange of the functionalities between the reactants, has been an important molecular transformation as complementary functionalization approaches toward established carbon framework building methods like cross-coupling reactions.[1–8] Recently, metathesis via C–S oxidative addition/reductive elimination to/from transition-metal catalysts has been attracting much attention as a functionalization of sulfur-containing molecules while the molecular frameworks are intact (Figure 1A)[9–19] because thioethers are widely seen in various chemistry fields including polymers, natural products, bioactive compounds, and pharmaceuticals.[20–22] Especially, C–S/C–Br metathesis between thioethers and bromoarenes is attractive based on the fact that bromoarenes represent one of the most useful functionalities because it offers various transformative functionalization into valuable compounds in addition to the importance of bromoarenes themselves in diverse fields of chemistry,[23–28] which is underpinned by the facile C–Br oxidative addition to transition-metal catalysts;[23,24,29] however, C–S/C–Br metathesis has not been reported so far despite its synthetic utility (Figure 1A).

The proposed reaction mechanism of C–S/C–Br metathesis is as follows: (i) oxidative addition of C–S and C–Br bonds to transition-metal catalysts respectively, (ii) transmetalation between the two kinds of oxidative adducts, and (iii) C–S and C–Br reductive elimination to afford the metathesis products (Figure 1B). Considering that reversible C–S oxidative addition/reductive elimination has been realized in the aforementioned several C–S metathesis reports (Figure 1A),[9–19] among the elementary reactions that constitute the C–S/C–Br metathesis, C–Br reductive elimination seems to be one of the most difficult steps to proceed. In the case of Pd-based catalysts, the C–Br oxidative adducts (C–Pd^{II}–Br complexes) are generally reluctant to proceed with reductive elimination due to the high stability of C–Pd^{II}–Br complexes (Figure 1C).[23,24,29] Sterically encumbered ligands, such as tri-*tert*-butylphosphine and Buchwald ligands, were reported to enable the thermodynamically and kinetically unfavorable reductive elimination from C–Pd^{II}–Br complexes (Figure 1C),[23,24,29,30–35] but they also inhibit other steps such as transmetalation between oxidative adducts.[36,37] In fact, Pd complexes with the aforementioned sterically hindered ligands did not catalyze the C–S/C–Br metathesis between *p*-tolyl sulfide (**1a**) and bromobenzene (**2b**) at all (Table S1). In the related works, Yamaguchi et al. reported novel thioether synthetic methodologies via aryl exchange between thioethers and (pseudo)halide compounds including haloarenes,[38] but the haloarene counterparts were not produced at all via the aryl exchange reactions probably due to the use of a stoichiometric amount of Zn to promote the catalyst turnover. Morandi and Lee developed intermolecular C–COCl/C–I metathesis between aroyl chlorides and aryl iodides via reversible C–I oxidative addition/reductive elimination using a Pd catalyst with a Xantphos (4,5-bis(diphenylphosphino)-9,9-dimethylxanthene)

ligand[39] (Arndtsen and Macias also reported the same reaction using almost the same catalytic system in the same period);[40] however, the transmetalation proceeded not via anion exchange between two Pd complexes but via C–P bond metathesis in one Pd complex enabled by reductive elimination to form phosphoniums with halide anions (Cl and I) using the non-innocent ligand working as a temporary aryl group storage unit,[39] which is considered to be difficult to be applied to C–S bond metathesis because of too strong interaction between thiolates and metal catalysts for reductive elimination to form the corresponding phosphoniums. Therefore, the construction of catalytic systems compatible for reversible C–Br reductive elimination/oxidative addition and fast transmetalation between two kinds of oxidative adducts is quite difficult, leading to no previous reports on the C–S/C–Br metathesis.

In this study, to achieve the unprecedented C–S/C–Br metathesis, we focused on an Au–Pd alloy nanoparticle catalyst as the novel catalytic system different from metal complex catalysts frequently used for the development of organic reactions. In our recent report, differently from previously reported Pd-complex-catalyzed indirect C–S/C–S metathesis of thioethers in the presence of strong base and thiol additives (successive thiol/thioether metathesis for the promotion of transmetalation steps),[8,10,12] we achieved direct C–S/C–S metathesis of diaryl thioethers by a TiO_2-supported Au−Pd alloy nanoparticle catalyst with the Au/Pd molar ratio of 4.4 ($Au_{4.4}$–Pd_1/TiO_2) without any additives, wherein the diluted Pd ensembles by alloying Au(0) species probably promoted the oxidative addition step of multiple thioethers to other Pd sites on the same nanoparticles and the transmetalation step via thiolate spill-over onto Au(0) species with suppressing the too strong π-adsorption of diaryl thioethers on Pd ensembles (Figure 1D).[19] In addition to the aforementioned functions, based on the previous reports that the decreased ensembles of active metal species exhibit a single atom-like character,[41] we assumed that Pd active sites surrounded by Au metal atoms in the Pd–Au alloy nanoparticle catalysts were also possible to work like the Pd complex with sterically encumbered ligands, which would promote the C–Br reductive elimination on the Pd sites. Additionally, Sakurai et al. reported that oxidative addition of C−Cl bonds could be promoted by spill-over of Cl species to Au(0) species on Au−Pd alloy nanoparticles[42] and that C−Cl oxidative adducts to Pd(0) species in Au−Pd alloy nanoparticles were reluctant to leach into the reaction solutions via spill-over of Cl species onto Au(0) species.[43] Thus, we hypothesized that Au−Pd alloy nanoparticles can facilitate oxidative addition/reductive elimination of C–S and C–Br bonds without inhibiting the transmetalation steps thanks to the spill-over of thiolates and Br species on the Au−Pd alloy nanoparticle surface to achieve unprecedented C–S/C–Br metathesis.

Herein, we have developed C–S/C–Br metathesis between thioethers and bromoarenes for the first time in the presence of $Au_{4.4}$–Pd_1/TiO_2 (Figure 1E). $Au_{4.4}$–Pd_1/TiO_2 was proved to function as a heterogeneous catalyst and could be reused several times. This catalytic system was applicable to

different thioethers and bromoarenes to afford both aryl-exchanged thioethers and bromoarenes in high yields. In addition, this catalytic system enabled late-stage bromination of various thioethers possessing bioactive structures and polyphenylene sulfide (PPS) depolymerization via C–S/C–Br metathesis. The reaction mechanism involved in reversible C–S and C–Br oxidative addition/reductive elimination was corroborated by several control experiments combined with density functional theory (DFT) calculations using $Au_{18}Pd_2$ cluster models, which suggested that this unprecedented reaction is enabled by the characteristics specific to bimetallic alloy nanoparticle catalysts utilizing multiple adsorption/active sites on the surface: multiple oxidative addition, spill-over of anion species, and reductive elimination assisted by steric hinderance of adsorbed thioether-derived species.

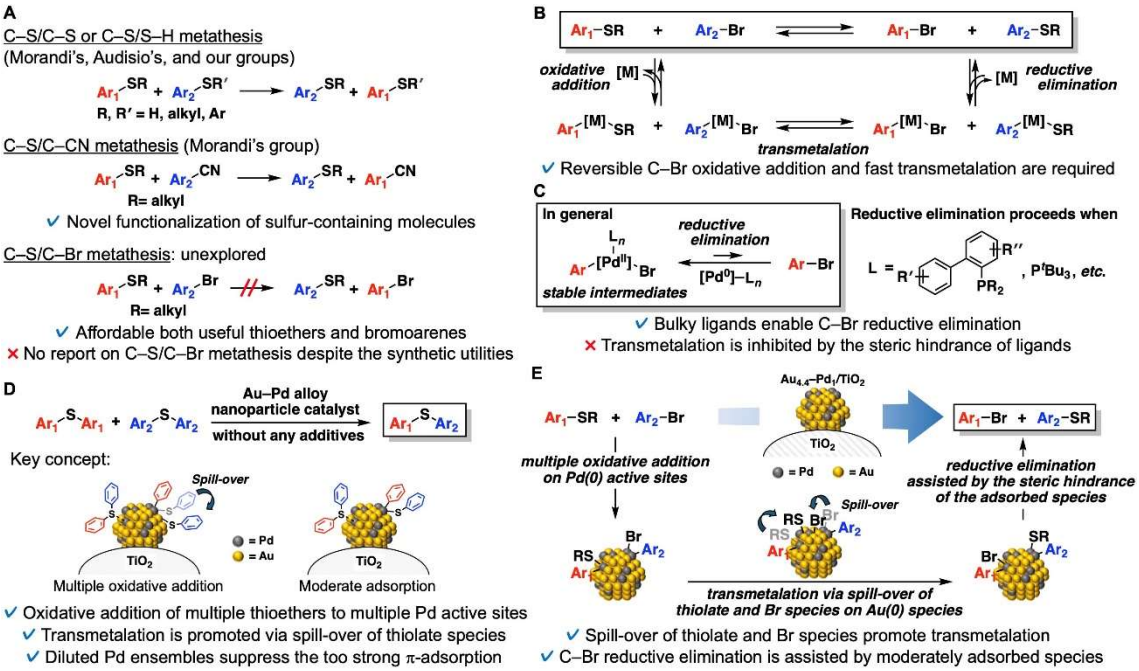

Figure 1. Background and overview of this study

(A) Metathesis involved in C–S oxidative addition/reductive elimination.

(B) Proposed reaction mechanism of C–S/C–Br metathesis.

(C) Difficult construction of catalytic systems compatible for C–Br reductive elimination and fast transmetalation.

(D) Our report on direct C–S/C–S metathesis of thioethers by an Au–Pd alloy nanoparticle catalyst.

(E) This study: C–S/C–Br metathesis enabled by an Au–Pd alloy nanoparticle catalyst.

RESULTS AND DISCUSSION

Effect of catalysts and optimization of conditions

We initially investigated the effect of the catalysts on the C−S/C−Br metathesis between thioethers and bromoarenes using **1a** and **2b** as the model substrates under the reaction conditions indicated in Table 1. Supported metal nanoparticle catalysts were prepared based on our previous report via deposition-precipitation of metal species on supports followed by $NaBH_4$ reduction (see Supplemental Information (SI) for the details of catalyst preparation).[19] When a TiO_2-supported monometallic Pd nanoparticle catalyst (Pd_1/TiO_2) was used as the catalyst, phenyl *p*-tolyl sulfide (**1ab**) and 4-bromotoluene (**2a**) were obtained in 6% and 11% yields, respectively (Table 1, entry 1). Pd complexes with various ligands (Table S1) and other supported metal species including Ni, Ru, Rh, Ir, Pt, or Au were not effective at all (Table 1, entries 2−7). Additionally, a TiO_2-supported Pd hydroxide ($Pd_1(OH)_x/TiO_2$) did not afford the metathesis products, suggesting that zero-valent Pd species are the active species for the present metathesis (Table 1, entry 8). On the basis of the strategies mentioned in the introduction part, we hypothesized the C−S/C−Br metathesis could be promoted in the presence of Au−Pd alloy nanoparticle catalysts. As we anticipated, $Au_{4.4}$–Pd_1/TiO_2, of which the alloy nanoparticle structure with mean diameter: 3.1 nm (σ = 0.8 nm) was confirmed by various characterizations as shown in SI (Figures S1–S6 and Table S2), exhibited much higher catalytic activities, producing **1ab** and **2a** in 36% and 44 % yields, respectively, concomitantly with the slight amount of phenyl sulfide (**1b**) (Table 1, entry 9). When TiO_2-supported Au−Pd alloy nanoparticle catalysts with various Au/Pd ratios were investigated, the yields of **1ab** and **2a** were higher as the Au/Pd ratio increased (Table S3). Other supports, such as Mg_3Al–CO_3-layered double hydroxide (LDH), ZrO_2, Al_2O_3, and hydroxyapatite (HAP) were comparatively ineffective for the present metathesis (Table S4). A physical mixture of $Au_{1.6}/TiO_2$ and Pd_1/TiO_2 slightly improved the **1ab** and **2a** yields (Table 1, entry 10). One of the possible reasons for the improved **1ab** and **2a** yields by the physical mixing of $Au_{1.6}/TiO_2$ and Pd_1/TiO_2 was that Pd species leached from Pd_1/TiO_2 deposited on $Au_{1.6}/TiO_2$ to form Au−Pd alloy nanoparticles during the reaction.[43,44] Through investigations of the catalysts and the reaction conditions including alloy partners (Table S5), solvents (Table S6), and reaction temperatures (Table S7), **1ab** and **2a** were obtained in 69% and 71% yields, respectively, in the presence of $Au_{4.4}$–Pd_1/TiO_2 (Table 1, entry 11). When increasing the **1a**/**2b** ratio (Table S8), the yields of **1ab** and **2a** reached up to 84% and 81%, respectively (Table 1, entry 12). The C–S/C–Br metathesis between **1a** and **2b** immediately stopped after the removal of the catalyst by hot-filtration during the reaction (Figure S7), and Au and Pd species were not detected in the filtrate after the hot-filtration by inductively coupled plasma–atomic emission spectroscopy (ICP-AES) analysis, confirming the observed catalysis was truly heterogeneous. $Au_{4.4}$–Pd_1/TiO_2 could be reused at least 5

times without significant loss of the final **1ab** and **2a** yields after catalyst regeneration via calcination at 300 °C for 3 h followed by reduction in water using $NaBH_4$ (Figure S8).

Table 1. Effect of catalysts on the C–S/C–Br metathesis of 1a and 2b.[a]

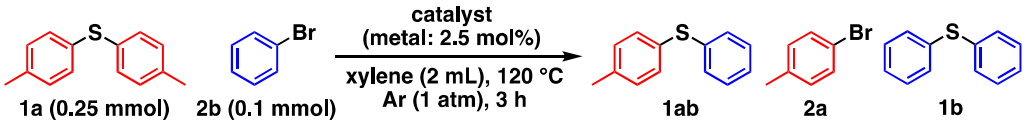

1a (0.25 mmol) 2b (0.1 mmol) 1ab 2a 1b

entry	catalyst	conv. (%)		yield (%)		
		1a	**2b**	**1ab**	**2a**	**1b**
1	Pd_1/TiO_2	17	22	6	11	<1
2[b]	Ni_5/TiO_2	13	7	<1	<1	<1
3	Ru_1/TiO_2	30	6	<1	<1	<1
4	Rh_1/TiO_2	33	<1	<1	<1	<1
5	Ir_1/TiO_2	11	5	<1	<1	<1
6	Pt_1/TiO_2	12	3	<1	<1	<1
7[c]	$Au_{1.6}/TiO_2$	13	10	<1	<1	<1
8	$Pd_1(OH)_x/TiO_2$	13	19	<1	<1	<1
9[d,e]	$Au_{4.4}$–Pd_1/TiO_2	35	56	36	44	7
10[c,d]	$Au_{1.6}/TiO_2$ + Pd_1/TiO_2	28	37	16	18	4
11[d,f]	$Au_{4.4}$–Pd_1/TiO_2	31	87	69	71	12
12[d,f,g]	$Au_{4.4}$–Pd_1/TiO_2	16	93	84	81	7

[a]Reaction conditions: **1a** (0.25 mmol), **2b** (0.1 mmol), catalyst (metal: 2.5 mol%), xylene (2 mL), Ar (1 atm), 120 °C, 3 h in test tube. Conversions and yields were determined by GC analysis using 1,3,5-trimethoxybenzene as an internal standard. [b]Ni: 5 mol%. [c]Au: 4 mol%. [d]Pd: 2.5 mol%. [e]Average of two runs is shown. [f]140 °C, 24 h. [g]**1a** (0.5 mmol).

Substrate scope

Substrate scope for $Au_{4.4}$–Pd_1/TiO_2-catalyzed C–S/C–Br metathesis between diaryl thioethers and bromoarenes was summarized in Figure 2. The structural formula of the used substrates and the substrate/product distributions including thioether byproducts were summarized in Figure S9 and Table S9, respectively. We initially investigated the substrate scope of thioethers (Figure 2A). This catalytic system was applicable to methyl-substituted diaryl thioethers regardless of the positions (**1ab**, **2a**; **1cb**, **2c**; **1db**, **2d**). *p*-Phenyl groups (**1eb**, **2e**) and electron-donating *p*-methoxy groups (**1fb**, **2f**) can be utilized in this catalytic system. Surprisingly, diaryl thioethers with fluoro or chloro groups went well to afford the corresponding unsymmetrical thioethers and bromoarenes without cleavage of fluoro or chloro groups (**1gb**, **2g**; **1hb**, **2h**). Diaryl thioethers with strong electron-withdrawing groups including *p*-trifluoromethyl (**1ib**, **2i**), *p*- or *m*-cyano (**1jb**, **2j**; **1kb**, **2k**), *p*- or *m*-acetyl (**1lb**, **2l**; **1mb**, **2m**), *p*-ethyl ester (**1nb**, **2n**), and *p*-nitro groups (**1ob**, **2o**), which make it hard to proceed with reductive elimination from C–Pd^{II}–Br species, can be subjected to the present metathesis in moderate to good yields. In the case of an alkyl aryl thioether, the C(sp^2)–S bromination occurred to produce the aryl-exchanged bromoarene while the counterpart (aryl-exchanged alkyl aryl thioether) could not be obtained (Figure S10). Although this reaction is not the C–S/C–Br metathesis, this catalytic system enables a quite useful selective transformation of C(sp^2)–S bonds toward C(sp^2)–Br bonds, which has not been achieved using any reagents so far, to our knowledge.

We next explored the substrate scope of bromoarenes (Figure 2B). The C–S/C–Br metathesis efficiently proceeded when using electron-donating *p*-, *m*-, or *o*-methyl (**1ba**, **2b**; **1bc**, **2b**; **1bd**, **2b**) or *p*-methoxy-substituted bromobenzenes (**1bf**, **2b**) to produce unsymmetrically substituted diaryl thioethers and bromobenzene in good yields. Bromoarenes with electron-withdrawing groups including trifluoromethyl (**1bi**, **2b**), cyano (**1bj**, **2b**), acetyl (**1bl**, **2b**), or ester groups (**1bp**, **2b**) tolerated well, providing the metathesis products. 1- or 2-Naphthyl groups (**1bq**, **2b**; **1br**, **2b**) and boronic pinacol ester (Bpin) groups (**1bs**, **2b**) tolerated the present metathesis as exemplified by the production of the metathesis products in moderate to good yields. When 1,4- or 1,3-bromobenzene was used as the substrate, double-metathesis product 1,4-bis[(4-methylphenyl)thio]benzene or 1,3-bis[(4-methylphenyl)thio]benzene was obtained, respectively (**1ab'a**, **2b**; **1ab''a**, **2b**).

This catalytic system could be applied to large-scale synthesis, giving **1ba** and **2b** in excellent yields when starting from 20 mmol of **1b** and 8 mmol of **2a** (Figure 2C). In addition, by the present C–S/C–Br metathesis using the solvent amount of **2b**, polyphenylene sulfide (PPS, **1b′**), one of the super engineering plastics used in a variety of fields and generally difficult to be decomposed,[45,46] was successfully depolymerized into **1b** and 1,4-dibromobenzene (**2b′**) (Figure 2D), which could be regarded as the depolymerization into a monomer based on the fact that PPS is

typically manufactured by the reaction between 1,4-dichlorobenzene and Na_2S.[45,46] There are some previous reports including ours on depolymerization of PPS;[10,18,19,47,48] however, this is the first example of depolymerization into the monomer, which will be utilized as the chemical recycling method.

Based on the aforementioned results, we further investigated the late-stage C(sp^2)–S bromination of alkyl aryl thioethers possessing natural product and/or bioactive structures using $Au_{4.4}$–Pd_1/TiO_2 with an excess amount of 4-bromoanisole (**2f**) (Figure 3). As indicated in Figure 3A, aryl alkyl thioethers with estrone (**1A**), testosterone (**1B**), umbelliferone (**1C**), flavone (**1D**), and xylenol (**1E**) moieties were viable to C(sp^2)–S bromination via Br transfer from **2f**. Since bromo groups are easily subjected to further transformative functionalization, we examined C(sp^2)–S bromination of a bioactive molecule followed by Suzuki–Miyaura coupling in order to demonstrate the synthetic utilities of the present reaction. In fact, the methylthio group in the methyl ester of sulindac sulfide (**1F**), a pharmacologically active metabolite of a kind of nonsteroidal anti-inflammatory drug sulindac,[49,50] could be converted into bromo group to afford **1F-Br** in 27% isolated yield followed by Suzuki–Miyaura coupling to form the corresponding biphenyl (**1F′**) (Figure 3B).

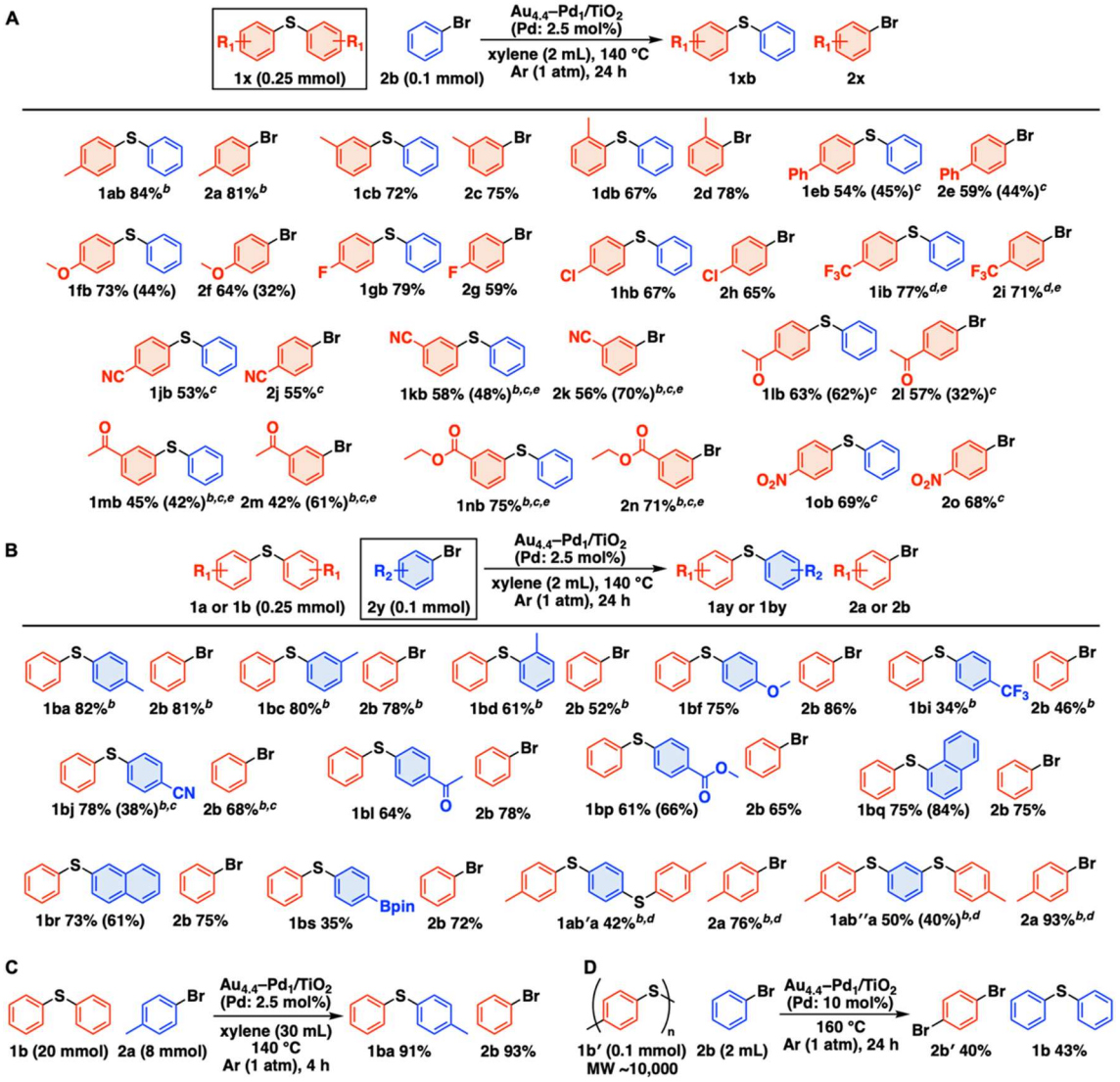

Figure 2. Substrate scope of this C–S/C–Br metathesis

(A) Scope of thioethers (**1x**).[a] [a]Reaction conditions: **1x** (0.25 mmol), **2b** (0.1 mmol), $Au_{4.4}$–Pd_1/TiO_2 (Pd: 2.5 mol%), xylene (2 mL), Ar (1 atm), 140 °C, 24 h in test tube. Yields based on **2b** were determined by GC analysis using 1,3,5-trimethoxybenzene as an internal standard. Values in parentheses are isolated yields. [b]**1x** (0.5 mmol). [c]$Au_{2.6}$–Pd_1/HAP (Pd: 5 mol%). [d]$Au_{4.4}$–Pd_1/TiO_2 (Pd: 5 mol%). [e]160 °C. HAP = hydroxyapatite.

(B) Scope of bromoarenes (**2y**).[a] [a]The reaction conditions are the same as shown above.

(C) Gram-scale reaction. The reaction conditions are indicated in the figure. GC yields using 1,3,5-trimethoxybenzene as an internal standard are shown.

(D) Depolymerization of PPS (**1b'**) to 1,4-dibromorbenzene (**2b'**) and **1b**. The reaction conditions are indicated in the figure. GC yields using 1,3,5-trimethoxybenzene as an internal standard are shown.

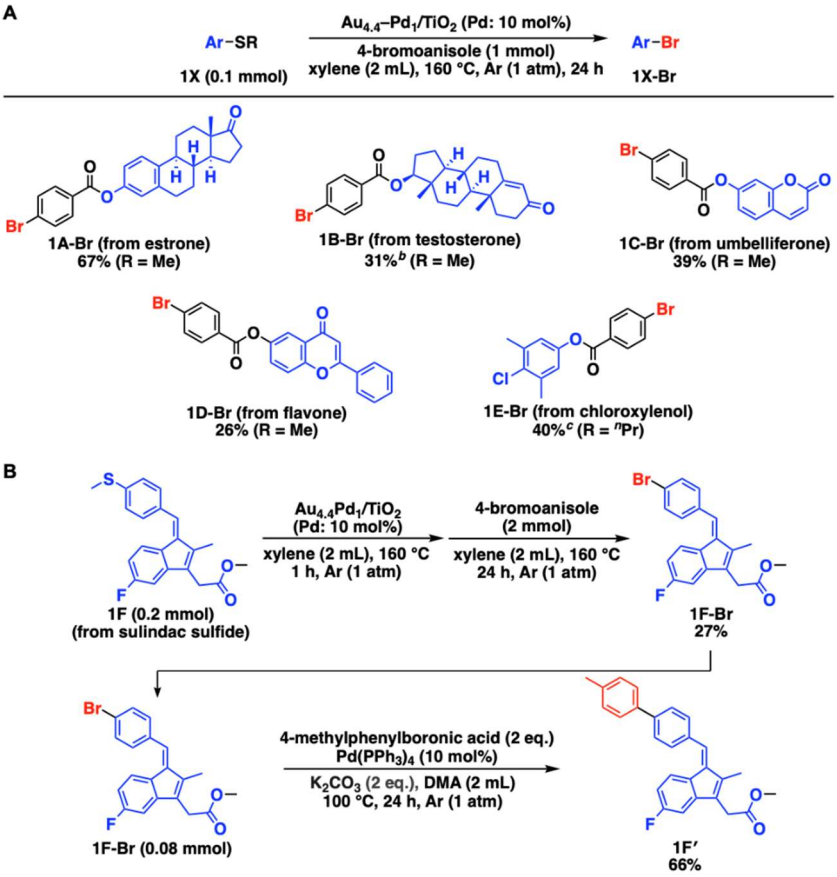

Figure 3. Substrate scope for the present C(sp^2)–S bromination of thioethers possessing bioactive structures

(A) Scope of thioethers possessing bioactive structures (**1X**).[a] [a]The reaction conditions are indicated in the figure. Isolated yields are shown. [b]NMR yield using 1,3,5-trimethoxybenzene as an internal standard is shown. [c]GC yield using 1,3,5-trimethoxybenzene as an internal standard is shown.

(B) Late-stage functionalization of the methyl ester of sulindac sulfide (**1F**) via the present C(sp^2)–S bromination followed by Suzuki–Miyaura cross-coupling. The reaction conditions are indicated in the figure. Isolated yields are shown.

Mechanistic studies

To obtain insights into the present reaction mechanism, we conducted several control experiments. First of all, to determine whether this reaction is reversible metathesis or not, the forward reaction (starting from **1a** (0.25 mmol) and **2b** (0.1 mmol)) and the reverse reaction (starting from **1a** (0.15 mmol), **1ab** (0.1 mmol), and **2a** (0.1 mmol)) were performed in the presence of $Au_{4.4}$–Pd_1/TiO_2. As a result, the detected amounts of **1a**, **2b**, **1ab**, **2a,** and **1b** after the forward reaction were almost the same as those after the reverse reaction (Table S10), confirming that the present reaction is reversible C–S/C–Br metathesis. Additionally, when 2,2,6,6-tetramethylpiperidine 1-oxyl (TEMPO) or 4-*tert*-butylcatechol (TBC) (0.15 mmol) was added as a radical scavenger into the forward reaction, the **1ab** and **2a** yields did not decrease so much, suggesting that radical species are not involved in the present C–S/C–Br metathesis (Table S11). Then, we examined the effect of the order of substrates added to the reaction solutions on the time-course plots of the C–S/C–Br metathesis. When 4-bromotoluene (**2a**) was injected after heating phenyl sulfide (**1b**) for 1 h in the presence of $Au_{4.4}$–Pd_1/TiO_2, the reaction profile was almost the same as that when **1b** and **2a** were placed in the reaction solution simultaneously (Figure S11). In contrast, a significant decrease in the yields of the metathesis products was observed when **2a** was heated with the catalyst prior to **1b** (Figure S12). Considering that $Au_{4.4}$–Pd_1/TiO_2 also catalyzed reversible C–S/C–S metathesis of thioethers[19] and that C–Br oxidative addition generally easily proceeds,[23,24,29] these results suggested that this C–S/C–Br metathesis efficiently proceeds after the preferential adsorption of thioethers over bromoarenes on the catalyst and that thioethers are difficult to access the surface covered with the excess amount of stable C–Br oxidative adducts, leading to the assumption that C–Br reductive elimination is promoted by the adsorption of thioethers on the catalyst.

Based on the aforementioned results, DFT calculations were performed to elucidate the reaction mechanism using Gaussian 16. By referring to the previous reports,[19,42,51–53] we adopted an $Au_{18}Pd_2$ cluster model for the calculation of the present C–S/C–Br metathesis catalytic cycle between phenyl sulfide (**1b**) and bromobenzene (**2b**) (Figure S13) using M06 functional with SDD basis sets for Au, Pd, and Br and 6-311G(d,p) basis sets for H, C, and S (see SI for the details of calculation methods). The overall Gibbs free energy diagram, the optimized structures, and the transition state structures were shown in Figures 4 and S14. Assuming that Pd is the active species for the oxidative addition/reductive elimination and that thioethers are preferentially adsorbed on the Pd sites over bromoarenes on the basis of the aforementioned experimental results, we initially adsorbed two molecules of **1b** on two Pd sites in the $Au_{18}Pd_2$ cluster (**Int 2**). Naturally, **Int 2** was more stable than the structure where one adsorbed **1b** was removed (**Int 1**). When one **1b** was replaced with one **2b** (**Int 3**), the structure was unstable compared with **Int 2**, which was consistent with the assumption of

preferential thioether adsorption over bromoarenes. Then, from **Int 3**, C–Br oxidative addition of **2b** proceeded to the Pd center via **TS 1**, where the neighboring Au was also slightly involved in the C–Br scission, to afford **Int 4**. As expected from the transition state structure, in **Int 4**, the Br anion was present in a bridged manner between two Au species, which could be called a kind of Br spill-over from Pd species to Au species. After slight migration (**Int 5**), C–S oxidative addition of the adsorbed **1b** proceeded via **TS 2** at the Pd center to form **Int 6**, and then, thiolate spill-over from the Pd species onto the neighboring Au species in the bridged manner (**Int 7**) and migration leaded to a local minimum (**Int 8**). Finally, C–Br reductive elimination from the phenyl species derived from **1b** on the Pd active site and the neighboring Br species bridged on the two Au species occurred via **TS 3** to afford **Int 9**. The desired aryl-exchanged bromoarene product can be obtained (**Int 10**) via facile desorption from **Int 9**. The activation free energies of **TS 1**, **TS 2**, and **TS 3** were calculated to be 17.6, 30.4, and 27.9 kcal/mol, respectively, which are considered to sufficiently proceed under the experimental conditions. Noteworthily, the reverse reaction from **Int 10** to **Int 1** along the aforementioned reaction coordinate using a bromoarene substrate instead of the aryl-exchanged bromoarene product affords the desired aryl-exchanged thioether counterpart and completes the catalytic cycle of the present C–S/C–Br metathesis. The activation free energies of **TS 1**, **TS 2**, and **TS 3** composed of the reverse reaction were also reasonable: 23.4, 25.0, and 22.7 kcal/mol, respectively. Remarkably, the respective activation free energies of oxidative addition and the corresponding reductive elimination were comparable (**TS 1**: 17.6 and 23.4 kcal/mol, **TS 2**: 30.4 and 25.0 kcal/mol, **TS 3**: 25.0 and 27.9 kcal/mol), indicating this C–S/C–Br metathesis can proceed reversibly. Therefore, the overall reaction coordinate (catalytic cycle) obtained by the DFT calculations using the $Au_{18}Pd_2$ cluster model is consistent with the experimental results on the present C–S/C–Br metathesis catalyzed by $Au_{4.4}$–Pd_1/TiO_2, which indicates that the formation of multiple oxidative adducts on the multiple isolated Pd sites in the same Au–Pd alloy nanoparticles and the transmetalation by spill-over of Br and thiolate anions on the surface through Au sites are the keys to achieving this unprecedented C–S/C–Br metathesis.

Finally, using the $Au_{18}Pd_2$ cluster model, we performed DFT calculations about the aforementioned assumption that C–Br reductive elimination can be promoted by the adsorption of thioethers on the Au–Pd alloy nanoparticle catalyst. The DFT calculation results of **2b** oxidative addition/reductive elimination at the Pd center of the $Au_{18}Pd_2$ cluster without **1b** adsorption (Figure S15) were compared with the aforementioned results of the same step in the presence of **1b** in Figure 5. The Gibbs free energy diagram revealed that the oxidative addition of **2b** was much easier in the absence of **1b** to proceed than the corresponding reductive elimination of **2b** (10.0 *vs* 28.4 kcal/mol) as with general oxidative addition of bromoarenes [23,24,29] despite almost the same transition

state structure (**TS 1'**) involved by the neighboring Au site as **TS 1** (Figure 5A). On the other hand, as shown above, the activation free energies of C–Br oxidative addition/reductive elimination with **1b** were comparable (17.6 *vs* 23.4 kcal/mol), and the C–Br reductive elimination was also indicated to be promoted by the adsorption of **1b** on the catalyst from the DFT calculation results (23.4 vs 28.4 kcal/mol) (Figure 5A). To reveal the origin of the C–Br reductive elimination promotion, we analyzed the natural-bond orbital (NBO) charges of the Pd (a) and Au (b and c) sites related to the reaction in the respective structures before/after the C–Br oxidative addition/reductive elimination (**Int 3**, **Int 4**, **Int 1'**, and **Int 2'**) (Figure 5B). As a result, the NBO charges of the Au sites hardly changed by the C–Br oxidative addition/reductive elimination albeit the presence of Br anions adsorbed on the Au sites. By contrast, the NBO charges of the Pd sites clearly increased after the C–Br oxidative addition in both of the cases, indicating the main active species for C–Br oxidative addition/reductive elimination is the Pd site. In addition, by the adsorption of **1b**, the NBO charges of the Pd sites involved in the C–Br oxidative addition/reductive elimination decreased, that is, the electrons at the Pd sites increased possibly via σ-donation from the S atom of **1b** to the adsorbed Pd atom[19] (**Int 3**: −0.919 *vs* **Int 1'**: −0.728, **Int 4**: −0.452 *vs* **Int 2'**: −0.429). In general, an electron-rich metal center has advantage in oxidative addition and inhibits reductive elimination.[54] Therefore, the electronic states could not explain why the C–Br reductive elimination was promoted by the adsorption of **1b**, and the other factor: steric hindrance from adsorbed **1b** should be the main reason for the promotion of C–Br reductive elimination by referring to the aforementioned metal complex cases realizing reductive elimination from C–Pd^{II}–Br complexes using sterically encumbered ligands.[23,24,29,30–35] In fact, the distance between the corresponding C atom and Br atom before C–Br reductive elimination was slightly shorter with the adsorption of **1b** than that without **1b** (Figure 5B). Thus, considering that too strong thioether adsorption will inhibit the access of bromoarenes to the catalyst in reverse and that thioether adsorption on Pd sites become much weaker by alloying with excess of Au than that on monometallic Pd species according to our previous report,[19] C–Br reductive elimination at Au-diluted Pd active sites assisted by the steric hindrance of thioethers (and C–S oxidative adducts) moderately adsorbed on the other nearby Pd (and Au) sites is also the key to the successful development of C–S/C–Br metathesis.

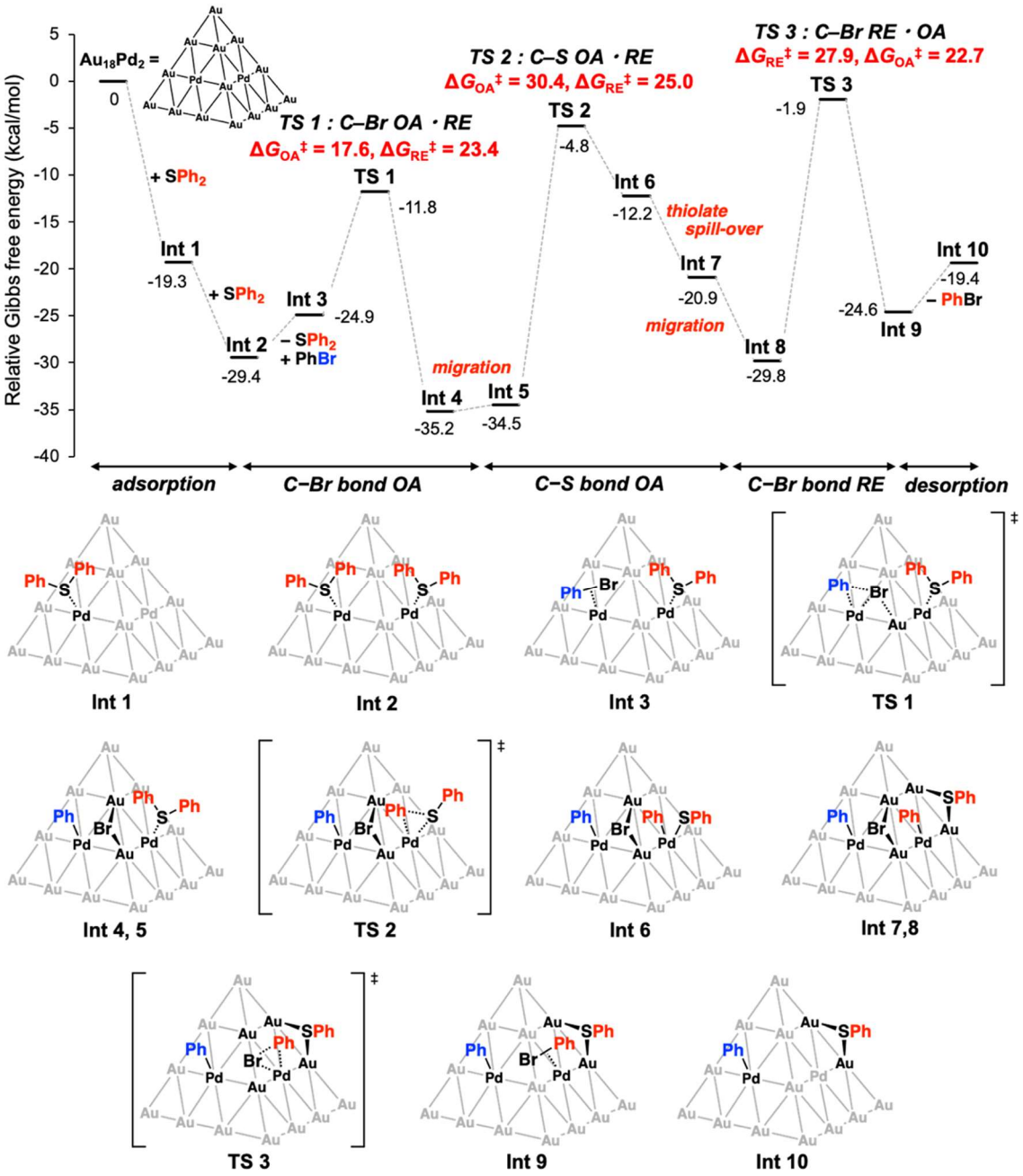

Figure 4. Overall Gibbs free energy diagram of the present C–S/C–Br metathesis between phenyl sulfide (**1b**) and bromobenzene (**2b**) and the corresponding optimized structures and transition states calculated using a $Au_{18}Pd_2$ cluster model. OA: oxidative addition. RE: reductive elimination.

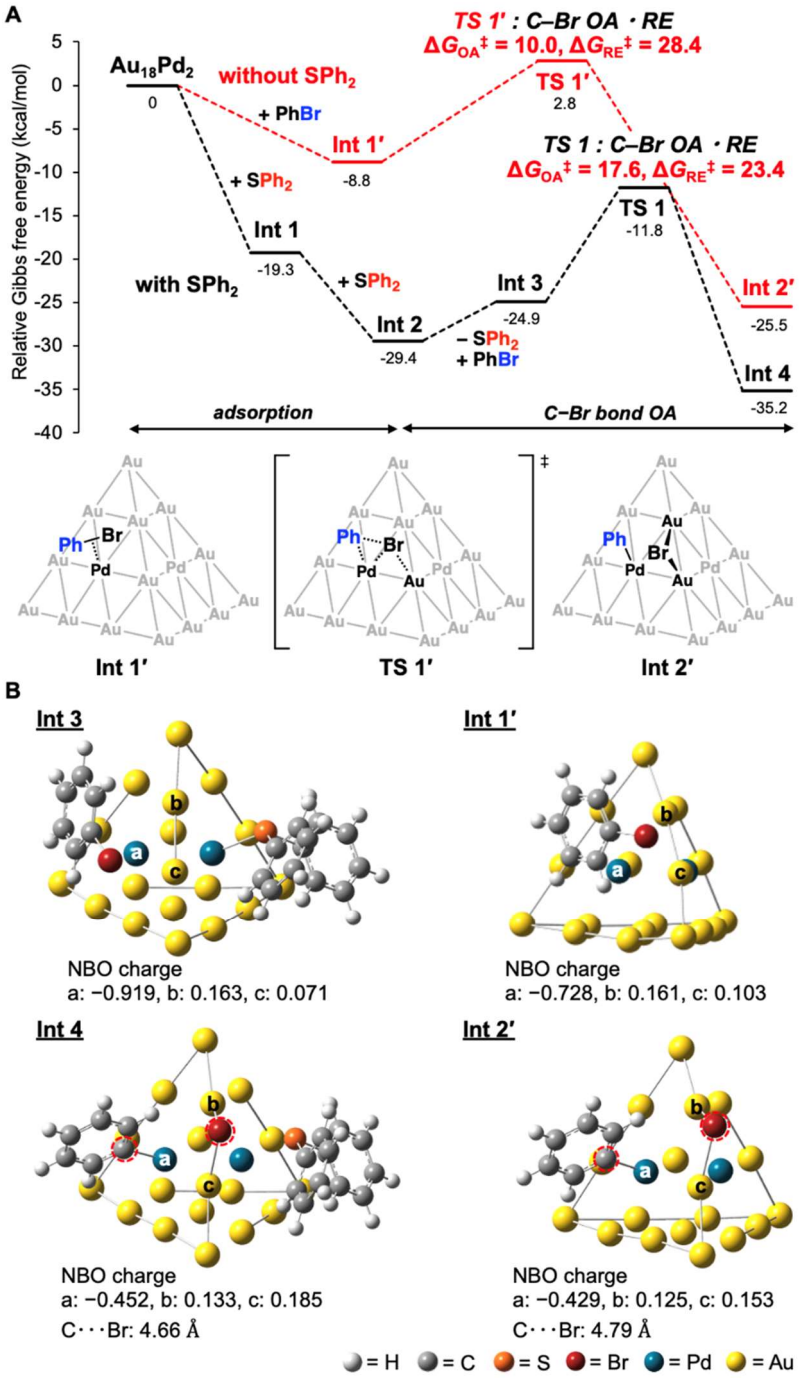

Figure 5. Comparison of C–Br oxidative addition/reductive elimination of bromobenzene (**2b**) with and without phenyl sulfide (**1b**) calculated using a $Au_{18}Pd_2$ cluster model.

(A) Gibbs free energy diagram along C–Br oxidative addition and the corresponding optimized structures and transition state without phenyl sulfide (**1b**).

(B) Optimized structures before and after the transition states of C–Br oxidative addition/reductive elimination with NBO charges of Pd and Au sites involved in the C–Br oxidative addition/reductive elimination.

Conclusions

In conclusion, we have successfully developed the first C–S/C–Br metathesis between thioethers and bromoarenes by using $Au_{4.4}$–Pd_1/TiO_2 as the reusable heterogeneous catalyst. This catalytic system exhibited various functional group tolerance and a broad substrate scope including late-stage transformations from C–S bonds to C–Br bonds in structurally diverse thioethers possessing bioactive structures and depolymerization of PPS to 1,4-dibromobenzene. Several control experiments and DFT calculations consistent with experimental results revealed that the construction of catalytic systems compatible for reversible C–Br bond oxidative addition/reductive elimination and fast transmetalation between the oxidative adducts, which are indispensable for achieving C–S/C–Br metathesis, was enabled by the characteristics specific to the present Au–Pd alloy nanoparticle catalyst with the high Au/Pd ratio: i) multiple reversible oxidative addition of C–S/C–Br bonds on the multiple isolated Pd sites in the same Au–Pd alloy nanoparticles, ii) transmetalation by spill-over of Br and thiolate anions on the surface through Au sites, and iii) C–Br reductive elimination assisted by the steric hindrance of thioether-derived species moderately adsorbed on the catalyst. We believe our catalytic system enabling the reversible C–S/C–Br metathesis, especially the C–Br reductive elimination without additional sterically hindered ligands, will be applied to other unprecedented catalytic functional group transformations, and exploring novel organic reactions by utilizing the unique catalysis and catalytic design is now underway.

EXPERIMENTAL PROCEDURES

Resource availability

Lead contact

Further information and requests for resources should be directed to and will be fulfilled by the lead contact, Kazuya Yamaguchi (kyama@appchem.t.u-tokyo.ac.jp).

Materials availability

All chemical materials and experimental/DFT calculation procedures in this study are summarized in the main text or supplemental information.

Data and code availability

All data related to the findings of this article are included in the main text or supplemental information. Additional data are available from the lead contact upon reasonable request.

SUPPLEMENTAL INFORMATION

Supplemental information can be found online.

ACKNOWLEDGMENTS

This work was financially supported by JSPS KAKENHI Grant No. 22H04971, 24K17556, 24H01062 (Transformative Research Areas (A) JP21A204), and 24H02210 (Transformative Research Areas (A) JP24A202). This work was supported by JST, PRESTO Grant Number JPMJPR227A, Japan. A part of this work was conducted at the Advanced Characterization Nanotechnology Platform of the University of Tokyo, supported by "Nanotechnology Platform" of the Ministry of Education, Culture, Sports, Science and Technology (MEXT), Japan. The computation was performed using Research Center for Computational Science, Okazaki, Japan (Project: 23-IMS-C002). T.M. was supported by the JSPS through the Research Fellowship for Young Scientists (Grant No. 23KJ0669). We thank Dr. Tomohiro Yabe for the help of XAFS measurements and analysis.

AUTHOR CONTRIBUTIONS

T.Y. and K.Y. conceived and supervised the project. T.M. performed most of the experiments. T.Y. conducted DFT calculations. All authors contributed to data analysis and discussed the results. T.M. and T.Y. wrote the manuscript with feedback from K.Y.

DECLARATION OF INTERESTS

The authors declare no competing interests.

REFERENCES

1. Fürstner, A. (2000). Olefin Metathesis and Beyond. Angew. Chem. Int. Ed. Engl. *39*, 3012–3043.

2. Grubbs, R.H. (2004). Olefin metathesis. Tetrahedron *60*, 7117–7140.

3. Fürstner, A. (2021). The Ascent of Alkyne Metathesis to Strategy-Level Status. J. Am. Chem. Soc. *143*, 15538–15555.

4. Estes, D.P., Bittner, C., Àrias, Ò., Casey, M., Fedorov, A., Tamm, M., and Copéret, C. (2016). Alkyne Metathesis with Silica-Supported and Molecular Catalysts at Parts-per-Million Loadings. Angew. Chem. Int. Ed. Engl. *55*, 13960–13964.

5. Diver, S.T., and Giessert, A.J. (2004). Enyne Metathesis (Enyne Bond Reorganization). Chem. Rev. *104*, 1317–1382.

6. Waterman, R. (2013). σ-Bond Metathesis: A 30-Year Retrospective. Organometallics *32*, 7249–7263.

7. Lin, Z. (2007). Current understanding of the σ-bond metathesis reactions of $L_nMR + R'–H \rightarrow L_nMR' + R–H$. Coord. Chem. Rev. *251*, 2280–2291.

8. Bhawal, B.N. and Morandi, B. (2019). Catalytic Isofunctional Reactions—Expanding the Repertoire of Shuttle and Metathesis Reactions. Angew. Chem. Int. Ed. Engl. *58*, 10074–10103.

9. Arisawa, M., Tagami, Y., and Yamaguchi, M. (2008). Two types of rhodium-catalyzed CS/CS metathesis reactions: formation of CS/CS bonds and CC/SS bonds. Tetrahedron Lett. *49*, 1593–1597.

10. Lian, Z., Bhawal, B.N., Yu, P., and Morandi, B. (2017). Palladium-catalyzed carbon-sulfur or carbon-phosphorus bond metathesis by reversible arylation. Science *356*, 1059–1063.

11. Delcaillau, T., Bismuto, A., Lian, Z., and Morandi, B. (2020). Nickel-Catalyzed Inter- and Intramolecular Aryl Thioether Metathesis by Reversible Arylation. Angew. Chem. Int. Ed. Engl. *59*, 2110–2114.

12. Rivero-Crespo, M.A., Toupalas, G., and Morandi, B. (2021). Preparation of Recyclable and Versatile Porous Poly(aryl thioether)s by Reversible Pd-Catalyzed C–S/C–S Metathesis. J. Am. Chem. Soc. *143*, 21331–21339.

13. Delcaillau, T., Boehm, P., and Morandi, B. (2021). Nickel-Catalyzed Reversible Functional Group Metathesis between Aryl Nitriles and Aryl Thioethers. J. Am. Chem. Soc. *143*, 3723–3728.

14. Boehm, P., Müller, P., Finkelstein, P., Rivero-Crespo, M.A., Ebert, M.-O., Trapp, N., and Morandi, B. (2022). Mechanistic Investigation of the Nickel-Catalyzed Metathesis between Aryl Thioethers and Aryl Nitriles. J. Am. Chem. Soc. *144*, 13096–13108.

15. Mouhsine, B., Norlöff, M., Ghouilem, J., Sallustrau, A., Taran, F., and Audisio, D. (2024). Platform for Multiple Isotope Labeling via Carbon–Sulfur Bond Exchange. J. Am. Chem. Soc. *146*, 8343–8351.

16. Bie, F., Liu, X., Cao, H., Shi, Y., Zhou, T., Szostak, M., and Liu, C. (2021). Pd-Catalyzed Double-Decarbonylative Aryl Sulfide Synthesis through Aryl Exchange between Amides and Thioesters. Org. Lett. *23*, 8098–8103.

17. Mitamura, K., Yatabe, T., Yamamoto, K., Yabe, T., Suzuki, K., and Yamaguchi, K. (2021). Heterogeneously Ni–Pd nanoparticle-catalyzed base-free formal C–S bond metathesis of thiols. Chem. Commun. *57*, 3749–3752.

18. Matsuyama, T., Yatabe, T., Yabe, T., and Yamaguchi, K. (2024). Direct thioether metathesis enabled by *in situ* formed Pd nanocluster catalysts. Catal. Sci. Technol. *14*, 76–82.

19. Matsuyama, T., Yatabe, T., Yabe, T., and Yamaguchi, K. (2024). Heterogeneously catalyzed thioether metathesis by a supported Au–Pd alloy nanoparticle design based on Pd ensemble control. Chem. Sci. *15*, 11884–11889.

20. Dunbar, K.L., Scharf, D.H., Litomska, A., and Hertweck, C. (2017). Enzymatic Carbon–Sulfur Bond Formation in Natural Product Biosynthesis. Chem. Rev. *117*, 5521–5577.

21. Ilardi, E.A., Vitaku, E., and Njardarson, J.T. (2014). Data-Mining for Sulfur and Fluorine: An Evaluation of Pharmaceuticals To Reveal Opportunities for Drug Design and Discovery. J. Med. Chem. *57*, 2832–2842.

22. Mutlu, H., Ceper, E.B., Li, X., Yang, J., Dong, W., Ozmen, M.M., and Theato, P. (2019). Sulfur Chemistry in Polymer and Materials Science. Macromol. Rapid Commun. *40*, 1800650.

23. Petrone, D.A., Ye, J., and Lautens, M. (2016) Modern Transition-Metal-Catalyzed Carbon–Halogen Bond Formation. Chem. Rev. *116*, 8003–8104.

24. Jones, D.J., Lautens, M., and McGlacken, G.P. (2019). The emergence of Pd-mediated reversible oxidative addition in cross coupling, carbohalogenation and carbonylation reactions. Nat. Catal. *2*, 843–851.

25. Voskressensky, L.G., Golantsov, N.E., and Maharramov, A.M. (2016). Recent Advances in Bromination of Aromatic and Heteroaromatic Compounds. Synthesis *48*, 615–643.

26. Knochel, P., Dohle, W., Gommermann, N., Kneisel, F.F., Kopp, F., Korn, T., Sapountzis, I., and Vu, V.A. (2003). Highly Functionalized Organomagnesium Reagents Prepared through Halogen–Metal Exchange. Angew. Chem. Int. Ed. Engl. *42*, 4302–4320.

27. Seechurn, C.C.C.J., Kitching, M.O., Colacot, T.J., and Snieckus, V. (2012). Palladium-Catalyzed Cross-Coupling: A Historical Contextual Perspective to the 2010 Nobel Prize. Angew. Chem. Int. Ed. Engl. *51*, 5062–5085.

28. Jiang, D.-B., Wu, F.-Y., and Cui, H.-L. (2023). Recent progress in the oxidative bromination of arenes and heteroarenes. Org. Biomol. Chem. *21*, 1571–1590.

29. Jiang, X., Liu, H., and Gu, Z. (2012). Carbon–Halogen Bond Formation by the Reductive Elimination of Pd^{II} Species. Asian J. Org. Chem. *1*, 16–24.

30. Shen, X., Hyde, A.M., and Buchwald, S.L. (2010). Palladium-Catalyzed Conversion of Aryl and Vinyl Triflates to Bromides and Chlorides. J. Am. Chem. Soc. *132*, 14076–14078.

31. Pan, J., Wang, X., Zhang, Y., and Buchwald, S.L. (2011). An Improved Palladium-Catalyzed Conversion of Aryl and Vinyl Triflates to Bromides and Chlorides. Org. Lett. *13*, 4974–4976.

32. Newman, S.G., and Lautens, M. (2010). The Role of Reversible Oxidative Addition in Selective Palladium(0)-Catalyzed Intramolecular Cross-Couplings of Polyhalogenated Substrates: Synthesis of Brominated Indoles. J. Am. Chem. Soc. *132*, 11416–11417.

33. Roy, A.H., and Hartwig, J.F. (2004). Reductive Elimination of Aryl Halides upon Addition of Hindered Alkylphosphines to Dimeric Arylpalladium(II) Halide Complexes. Organometallics *23*, 1533–1541.

34. Roy, A.H., and Hartwig, J.F. (2003). Directly Observed Reductive Elimination of Aryl Halides from Monomeric Arylpalladium(II) Halide Complexes. J. Am. Chem. Soc. *125*, 13944–13945.

35. Roy, A.H., and Hartwig, J.F. (2001). Reductive Elimination of Aryl Halides from Palladium(II). J. Am. Chem. Soc. *123*, 1232–1233.

36. Clarke, M.L., and Heydt, M. (2005). The Importance of Ligand Steric Effects on Transmetalation. Organometallics *24*, 6475–6478.

37. Ariafard, A., and Yates, B.F. (2009). Subtle Balance of Ligand Steric Effects in Stille Transmetalation. J. Am. Chem. Soc. *131*, 13981–13991.

38. Isshiki, R., Kurosawa, M.B., Muto, K., and Yamaguchi, J. (2021). Ni-Catalyzed Aryl Sulfide Synthesis through an Aryl Exchange Reaction. J. Am. Chem. Soc. *143*, 10333–10340.

39. Lee, Y.H., and Morandi, B. (2018). Metathesis-active ligands enable a catalytic functional group metathesis between aroyl chlorides and aryl iodides. Nat. Chem. *10*, 1016–1022.

40. Macias, M.D.L.H., and Arndtsen, B.A. (2018). Functional Group Transposition: A Palladium-Catalyzed Metathesis of Ar–X σ-Bonds and Acid Chloride Synthesis. J. Am. Chem. Soc. *140*, 10140–10144.

41. Greiner, M.T., Jones, T.E., Beeg, S., Zwiener, L., Scherzer, M., Girgsdies, F., Piccinin, S., Armbrüster, M., Knop-Gericke, A., and Schlögl, R. (2018). Free-atom-like *d* states in single-atom alloy catalysts. Nat. Chem. *10*, 1008–1015.

42. Dhital, R.N., Kamonsatikul, C., Somsook, E., Bobuatong, K., Ehara, M., Karanjit, S., and Sakurai, H. (2012). Low-Temperature Carbon–Chlorine Bond Activation by Bimetallic Gold/Palladium Alloy Nanoclusters: An Application to Ullmann Coupling, J. Am. Chem. Soc. *134*, 20250–20253.

43. Karanjit, S., Jinasan, A., Samsook, E., Dhital, R.N., Motomiya, K., Sato, Y., Tohji, K., and Sakurai, H. (2015). Significant stabilization of palladium by gold in the bimetallic nanocatalyst leading to an enhanced activity in the hydrodechlorination of aryl chlorides. Chem. Commun. *51*, 12724–12727.

44. Matsuyama, T., Yatabe, T., Yabe, T., and Yamaguchi, K. (2022). Decarbonylation of 1,2-Diketones to Diaryl Ketones via Oxidative Addition Enabled by an Electron-Deficient Au–Pd Nanoparticle Catalyst. ACS Catal. *12*, 13600–13608.

45. Rahate, A.S., Nemade, K.R., and Waghuley, S.A. (2013). Polyphenylene sulfide (PPS): state of the art and applications. Rev. Chem. Eng. *29*, 471–489.

46. Zuo, P., Tcharkhtchi, A., Shirinbayan, M., Fitoussi, J., and Bakir, F. (2019). Overall Investigation of Poly (Phenylene Sulfide) from Synthesis and Process to Applications—A Review. Macromol. Mater. Eng. *304*, 1800686.

47. Minami, Y., Matsuyama, N., Matsuo, Y., Tamura, M., Sato, K., and Nakajima, Y. (2021). Catalytic Reductive Cleavage of Poly(phenylene sulfide) Using a Hydrosilane. Synthesis *53*, 3351–3354.

48. Delcaillau, T., Woenckhaus-Alvarez, A., and Morandi, B. (2021). Nickel-Catalyzed Cyanation of Aryl Thioethers. Org. Lett. *23*, 7018–7022.

49. Nortcliffe, A., Ekstrom, A.G., Black, J.R., Ross, J.A., Habib, F.K., Botting, N.P., and O'Hagan, D. (2014). Synthesis and biological evaluation of nitric oxide-donating analogues of sulindac for prostate cancer treatment. Bioorg. Med. Chem. *22*, 756–761.

50. Williams, C.S., Goldman, A.P., Sheng, H., Morrow, J.D., and DuBois, R.N. (1999). Sulindac Sulfide, but Not Sulindac Sulfone, Inhibits Colorectal Cancer Growth. Neoplasia *1*, 170–176.

51. Lang, X.-F., Yin, P.-G., You, T.-T., and Guo, L. (2012). Chemical Effects in SERS of Pyrazine Adsorbed on Au–Pd Bimetallic Nanoparticles: A Theoretical Investigation. ChemPhysChem *13*, 237–244.

52. Miyazaki, R., Jin, X., Yoshii, D., Yatabe, T., Yabe, T., Mizuno, N., Yamaguchi, K., and Hasegawa, J. (2021). Mechanistic study of C–H bond activation by O_2 on negatively charged Au clusters: α,β-dehydrogenation of 1-methyl-4-piperidone by supported Au catalysts. Catal. Sci. Technol. *11*, 3333–3346.

53. Takei, D., Yatabe, T., Yabe, T., Miyazaki, R., Hasegawa, J., and Yamaguchi, K. (2022). C–H Bond Activation Mechanism by a Pd(II)–(μ-O)–Au(0) Structure Unique to Heterogeneous Catalysts. JACS Au *2*, 394–406.

54. Hartwig, J.F. (2007). Electronic Effects on Reductive Elimination To Form Carbon−Carbon and Carbon−Heteroatom Bonds from Palladium(II) Complexes. Inorg. Chem. *46*, 1936–1947.